Intramolecular Rearrangement for Regioselective Complexation by Intramolecular CH/π Interaction in a Hydrophobic Cavity of a Ruthenium Coordination Sphere

Takahiko Kojima,*[a] Soushi Miyazaki,[a] Ken-ichi Hayashi,[a] Yuichi Shimazaki,[b] Fumito Tani,[b] Yoshinori Naruta,[b] and Yoshihisa Matsuda[a]

Abstract: A Ru^{II} complex with a hydrophobic cavity formed from two 1-naphthoylamide groups was prepared. Its reactions with β-diketones gave β-diketonato complexes in which hydrophobic π–π or CH/π interactions were confirmed by NMR spectroscopy and X-ray crystallography. In the case of the asymmetric β-diketone benzoylacetone, an isomer with a CH/π interaction was afforded as the sole product owing to thermodynamic control. The reaction was found to involve a novel intramolecular rearrangement from the phenyl-included isomer to the methyl-included one without rupture of Ru–β-diketonato coordination bonds (activation energy 52 kJ mol^{-1}). This indicates that CH/π interactions can be more favored thermodynamically than π–π interactions in a suitable hydrophobic environment.

Keywords: ligand effects · N ligands · noncovalent interactions · rearrangement · ruthenium

Introduction

Noncovalent interactions play indispensable roles in biological systems in forming specific structures required for certain functions such as molecular recognition, and in performing selective chemical conversion of substrates in enzymatic reactions.[1] Among these, hydrophobic interactions such as CH/π[2] and π–π[3] interactions are recognized to be not as strong as hydrogen bonding; however, they also play an important role in those phenomena.[4] The π–π interaction has been recognized as a powerful tool for constructing supramolecular assemblies[5,6] and molecular recognition,[7] and as a strong driving force for interactions (intercalation) between DNA and pharmaceuticals such as bleomycin.[8] On the other hand, the CH/π interaction is known to play an important role in functionality, for example in the tumor suppressor protein p53,[9] in which the activity is attributed to a CH/π interaction between the phenyl group of phenylalanine and the S-methyl group of methionine.[10] With regard to organic reactions, Houk and co-workers have suggested that a CH/π interaction plays an important role in determining the stereoselectivity in a hetero-Diels–Alder reaction between *ortho*-xylylenes and aliphatic aldehydes.[11]

In the coordination sphere around a metal center, noncovalent interactions can also play major roles in determining its geometry, characteristics, reactivity, and selectivity.[12,13] Yamauchi[14] and Sigel[15] and their co-workers have extensively studied noncovalent interactions, in particular π–π interactions, in the coordination spheres of metal complexes. They have argued the importance of π–π interactions in terms of the specific orientation of the aromatic rings in ternary complexes in the presence of heteroaromatic ligands such as 2,2′-bipyridine and 1,10-phenanthroline. With regard to CH/π interactions in coordination spheres, Okawa and co-workers have reported that β-diketonato complexes having *l*-menthoxy moieties can be prepared stereoselectively due to interligand CH/π interactions.[16] They also took advantage of CH/π interactions in the enantioselective reduction of ketones with lanthanoid(III) complexes.[17]

We have synthesized a series of bisamide-TPA (TPA = tris(2-pyridylmethy)amine) ligands and their Ru^{II} complexes to investigate the ability of noncovalent interactions in coordination spheres to regulate the stereochemistry and chemical properties of Ru centers.[18] Herein, we describe the importance of CH/π interactions in determining the regioselec-

[a] Dr. T. Kojima, S. Miyazaki, K.-i. Hayashi, Prof. Y. Matsuda
Department of Chemistry, Faculty of Sciences, Kyushu University
Hakozaki, Higashi-Ku, Fukuoka 812–8581 (Japan)
Fax: (+81) 92-642-2570
E-mail: cosyscc@mbox.nc.kyushu-u.ac.jp

[b] Dr. Y. Shimazaki, Prof. F. Tani, Prof. Y. Naruta
Institute for Materials Chemistry and Engineering, Kyushu University, Hakozaki, Higashi-Ku, Fukuoka 812–8581 (Japan)

Supporting information for this article is available on the WWW under http://www.chemeurj.org/ or from the author. CIF files for **2**, **3**, and $\mathbf{4}_{Me}$, VT–^{1}H NMR spectra for **2** and **3**, differential ^{1}H NOE spectrum for **3**, UV/Vis spectra of **1**–**4** in CH_3CN, a part of ^{1}H NMR spectrum of the mixture of **4**.

DOI: 10.1002/chem.200400496

tivity around the metal center after a thermodynamic intramolecular rearrangement.

Results and Discussion

Reactions of 1 with β-diketones: The reactions of the ruthenium complex **1**[19] with β-diketones described herein are summarized in Scheme 1. The reaction mixture of **1** and

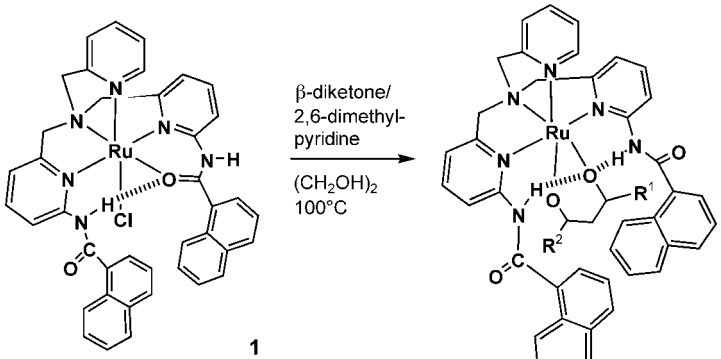

Scheme 1. Synthesis of β-diketonato complexes.

Hdbm (dibenzoylmethane) needed to be heated to 100 °C for 45 h in ethylene glycol to afford $[Ru(dbm)(L)]^+$ (**2**) (L = 1-$Naph_2$-TPA). In the course of the reaction, the UV spectrum of reaction mixture revealed a evolution of an absorption at 456 nm, which was assigned to a ligand-to-metal charge-transfer (LMCT) band from dbm^- to the Ru^{II} center (See Figure S4 in the Supporting Information). We also found that the reaction proceeds better and cleaner under N_2 than under air, probably due to oxidative degradation of coordinated β-diketonates by O_2. The ESI mass spectrum of **2** in CH_3CN exhibited a peak cluster due to the molecular ion M^+ at 953.3, which was consistent with its simulated isotopic pattern.

The ^1H NMR spectrum of **2** in CD_3CN suggested that the molecule has a σ_h-symmetry since one singlet appeared at $\delta = 4.50$ ppm, which was assigned to the methylene protons of the axial pyridylmethyl arm, and one AB quartet appeared at $\delta = 4.78$ and 5.27 ppm ($J_{A,B} = 15$ Hz).[20] These results clearly indicate that the amide CO moiety is not bound to the Ru center any more in **2** and that the two 1-naphthoylamide groups are uncoordinated, leading to a hydrophobic cavity. The signals due to one of the phenyl moieties of the dbm^- ligand were observed at $\delta = 6.50$ (dd, 8 and 1 Hz; *o*-H), 5.54 (t, 8 Hz; *m*-H), and 6.12 ppm (td, 7 and 1 Hz; *p*-H) and they showed large upfield shifts relative to free dbm^-. These data indicate that one phenyl ring of dbm^- ligand is located in between the two 1-naphthyl moieties of L and enjoys free rotation based on the symmetric pattern of the phenyl group.

The reaction of **1** with acetylacetone (Hacac) in ethylene glycol at 100 °C gave the acetylacetonato complex [Ru(acac)(L)]PF_6 (**3**) in moderate yield. The ^1H NMR spectrum of **3** in CD_2Cl_2 showed one singlet and one AB quartet due to the axial and equatorial methylene protons, respectively, indicating that the coordinated amide moiety was released to form a σ_h-symmetric environment as observed in **2**. In addition, a singlet due to one of methyl groups of the $acac^-$ ligand exhibited a large upfield shift to $\delta = -0.27$ ppm compared to that ($\delta = 1.86$ ppm) of the other methyl group. This clearly shows that one methyl group was shielded by the naphthyl π-electron clouds. A differential NOE experiment on **3** upon irradiation of the singlet at $\delta = -0.27$ ppm in CD_2Cl_2 clearly showed close contacts among the included methyl group and naphthyl moieties of L (see Figure S3 in Supporting Information).

To illustrate the selectivity between a π–π interaction and a CH/π interaction, benzoylacetone (Hbac) was employed which contains both methyl and phenyl groups in the same molecule. The reaction of **1** with Hbac in ethylene glycol in the presence of 2,6-dimethylpyridine was monitored by UV/Vis spectroscopy, which revealed the evolution of an absorption at 440 nm due to the LMCT band from bac^- to the Ru^{II} center (See Figure S4 in Supporting Information). The reaction (4 h) gave a mixture of two isomers ($\mathbf{4_{Me}}$ and $\mathbf{4_{Ph}}$; Scheme 1). The ^1H NMR spectrum of the mixture of the two isomers showed a pattern of signals that were assigned to the methylene protons of the TPA ligand, which was similar to that observed in **2** and **3**. This indicates that the complex **4** has σ_h symmetry, demonstrating the coordinated amide became unbound to the Ru^{II} center. The ESI mass spectrum of **4** in CH_3CN showed peaks due to the M^+ ion with an isotopic pattern, which was consistent with a computer simulation. In the structure of $\mathbf{4_{Me}}$, the methyl group of bac^- is located in between the two 1-naphthyl groups, whereas the phenyl group of bac^- is located there in $\mathbf{4_{Ph}}$. In the ^1H NMR spectrum of a mixture of $\mathbf{4_{Ph}}$ and $\mathbf{4_{Me}}$ in $CD\mathbf{Cl}_3$, a singlet assigned to the methyl group of bac^- in $\mathbf{4_{Me}}$ was ob-

Abstract in Japanese:

２つの１－ナフトイルアミド基を有するトリス（２―ピリジルメチル）アミン(TPA)誘導体を配位子とするルテニウム(II)錯体([RuCl(1-$Naph_2$-TPA)]$^+$)は、β―ジケトンと反応して[Ru(β-diketonato)(1-$Naph_2$-TPA)]$^+$を与えた。このとき、２つの１－ナフチル基が構築する疎水場において、β―ジケトナト配位子の置換基との間でπ－πもしくは CH／π相互作用が発現する。一方、フェニル基とメチル基を有する非対称β―ジケトンを反応させた場合、配位結合の切断を伴わない新規な分子内転移反応（活性化エネルギー；５２ kJ mol^{-1}）を経由して、メチル基包摂体のみを生成した。このことは、CH／π相互作用がπ－π相互作用を熱力学的に凌駕する可能性を示しており、タンパク質などで見られる CH／π相互作用の重要性を支持する。

served at $\delta = -0.10$ ppm due to the ring current effect of the two 1-naphthyl moieties of L. The methyl peak for $\mathbf{4}_{Ph}$ was observed at $\delta = 2.07$ ppm, similar to that of **3**. The methine protons of bac$^-$ were observed at $\delta = 5.95$ and 5.78 ppm as singlets for $\mathbf{4}_{Ph}$ and $\mathbf{4}_{Me}$, respectively. Singlets at $\delta = 4.58$ and 4.60 ppm were assigned to the CH_2 protons of the axial pyridyl methylene arms for $\mathbf{4}_{Me}$ and $\mathbf{4}_{Ph}$, respectively. Signals assigned to the included phenyl protons of $\mathbf{4}_{Ph}$ were observed at $\delta = 5.56$ (t, $J = 8$ Hz 2H; *m*-H), 6.10 (t, $J = 7$ Hz, 1H; *p*-H), and 6.23 ppm (d, $J = 7$ Hz, 2H; *o*-H). These values were comparable to those of the included phenyl moiety in **2** (See Supporting Infromation; Figure S5). This observation confirms that the structure of $\mathbf{4}_{Ph}$ has the included phenyl group in the hydrophobic cavity.

Molecular structures of Ru^{II}-β-diketonato complexes: To gain additional convincing evidence for the presence of hydrophobic interactions in the complexes, crystal structures of **2**, **3**, and $\mathbf{4}_{Me}$ were determined by X-ray crystallography. ORTEP drawings of those structures are depicted in Figure 1, Figure 2, and Figure 3, respectively, together with selected bond lengths [Å] and angles [°]. In spite of a number of attempts, the data were not good enough to allow us to discuss on the details of the molecular structures; however, they were sufficient to provide support for our assumption of the existence of noncovalent interactions between the two 1-naphthyl groups and a functional group inserted between them in the hydrophobic cavity. The noncovalent interactions among the two 1-naphthyl groups and the phenyl group of **2** or the methyl groups of **3** and $\mathbf{4}_{Me}$ are shown in Figure 4a–c, respectively. Tables 1–3 list interatomic distances that indicate the occurrence of intramolecular

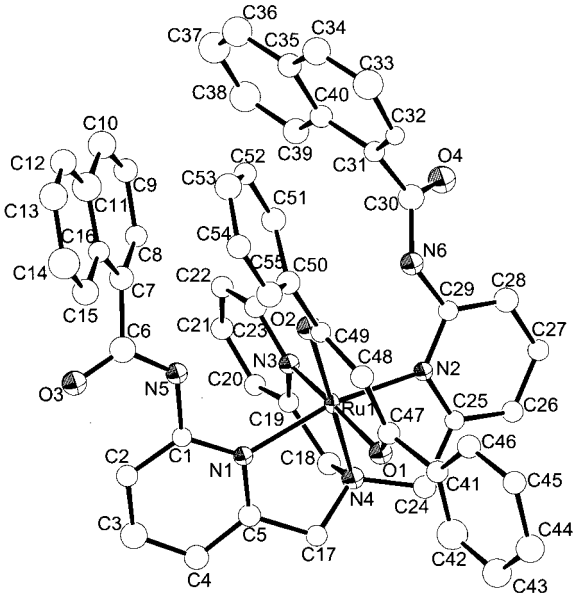

Figure 1. Molecular structure of **2** (ORTEP drawing with 50% probability thermal ellipsoids). Selected bond lengths [Å] and angles [°]: Ru1–O1 2.077(11), Ru1–O2 2.103(11), Ru1–N1 2.127(11), Ru1–N2 2.114(11), Ru1–N3 2.023(13), Ru1–N4 2.045(13); O1-Ru1-O2 90.6(4), N1-Ru1-N4 82.0(5), N2-Ru1-N4 80.4(5), N3-Ru1-N4 83.7(5), N1-Ru1-N2 161.8(4).

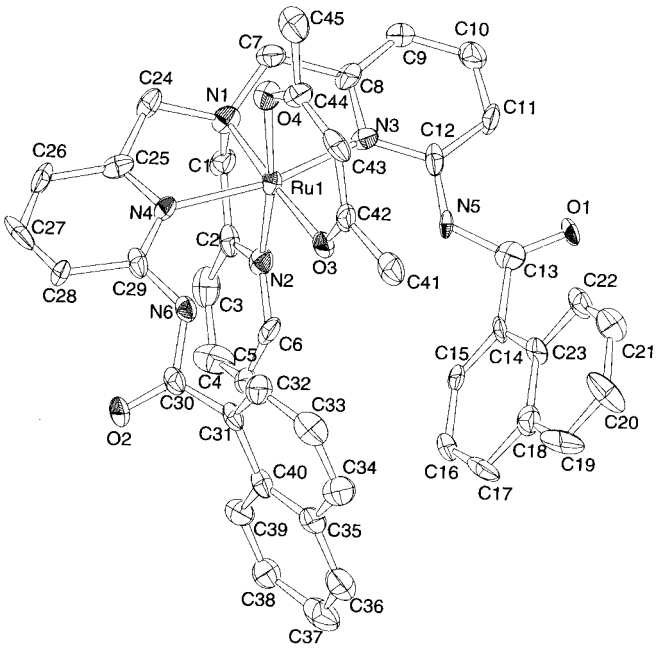

Figure 2. Molecular structure of **3** (ORTEP drawing with 30% probability thermal ellipsoids). Selected bond lengths [Å] and angles [°]: Ru1–O3 2.070(8), Ru1–O4 2.05(1), Ru1–N1 2.046(10), Ru1–N2 2.04(1), Ru1–N3 2.084(9), Ru1–N4 2.082(9); O3-Ru1-O4 91.0(4), O3-Ru1-N1 178.0(3), O4-Ru1-N4 171.1(4), N1-Ru1-N2 83.1(5), N1-Ru1-N3 80.3(4), N1-Ru1-N4 84.5(4), N3-Ru1-N4 164.8(4).

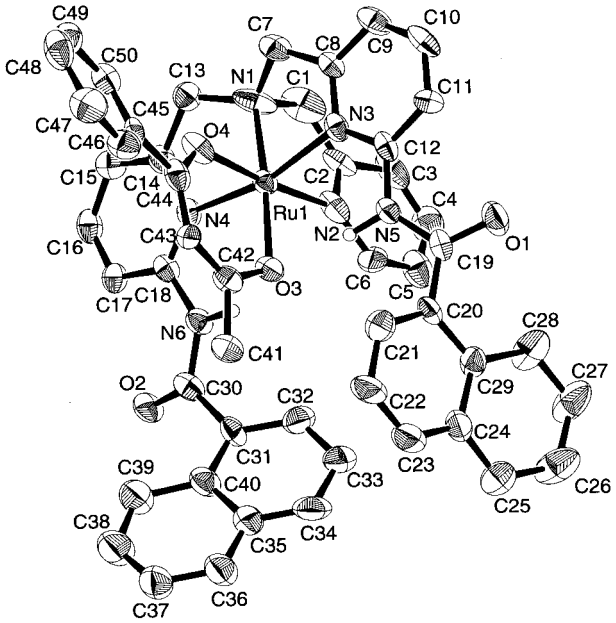

Figure 3. Molecular structure of $\mathbf{4}_{Me}$ (ORTEP drawing with 30% probability thermal ellipsoids). Selected bond lengths [Å] and angles [°]: Ru1–O3 2.139(8), Ru1–O4 2.063(8), Ru1–N1 2.002(10), Ru1–N2 2.04(1), Ru1–N3 2.100(8), Ru1–N4 2.115(9); O3-Ru1-O4 88.7(3), N1-Ru1-N2 88.6(5), N1-Ru1-N3 81.7(4), N1-Ru1-N4 82.6(4), N3-Ru1-N4 164.3(4).

π–π interactions for **2**, and CH/π interactions for **3** and $\mathbf{4}_{Me}$. The separation of the included functional groups from the centroids of the naphthyl moieties is also shown in

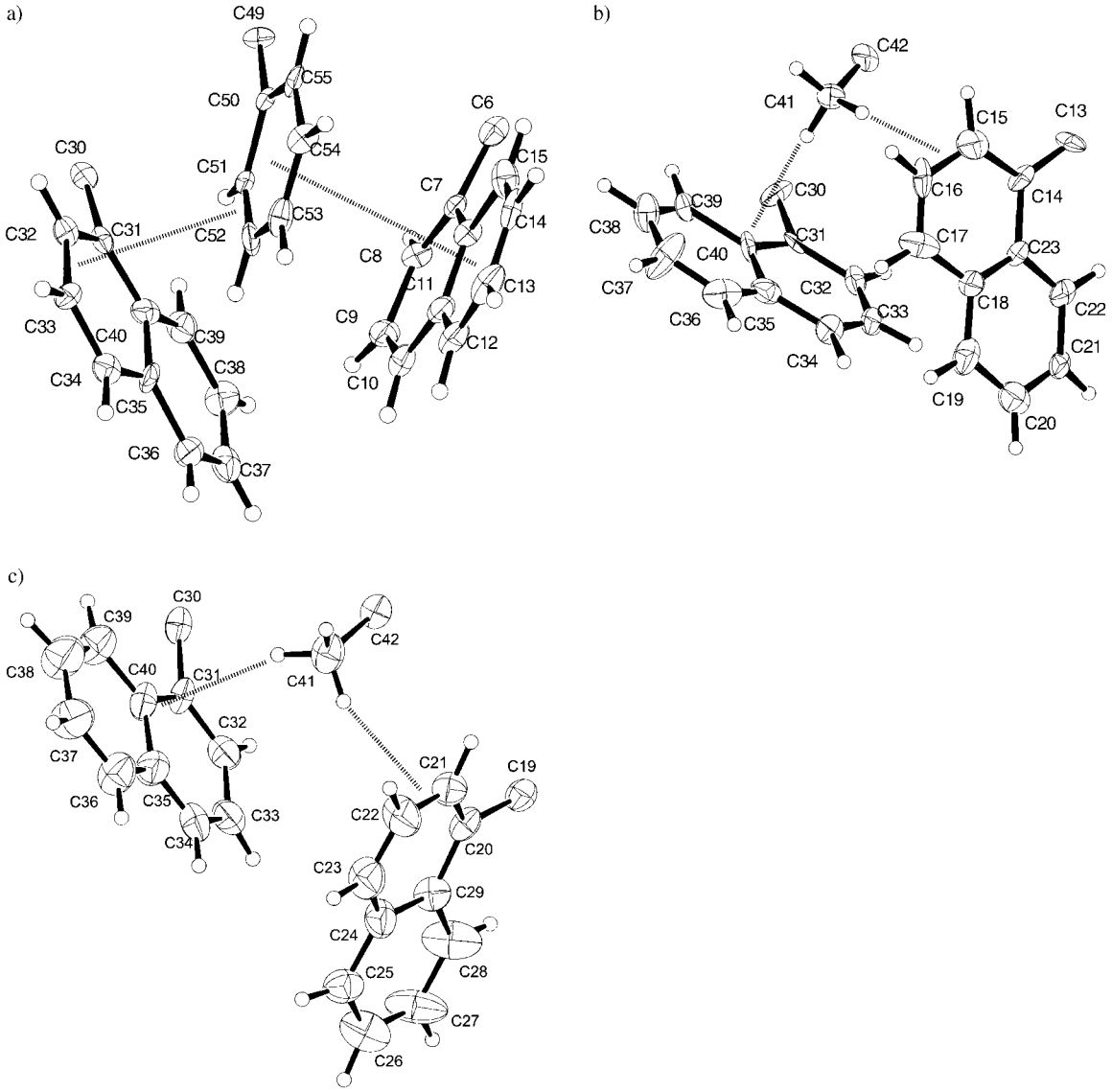

Figure 4. Partial ORTEP representations for noncovalent interactions in **2** (a), **3** (b), and $\mathbf{4}_{Me}$ (c). Thermal ellipsoids are shown at the 30% probability level.

Table 1. Interatomic distances [Å] for intramolecular π–π interactions and hydrogen bonding in **2**.

π–π interactions			
C53–C11	3.35	C53–C12	3.43
C53–C13	3.62	C53–C14	3.74
C53–C15	3.69	C53–C16	3.45
C52–C7	3.74	C52–C8	3.77
C52–C9	3.55	C52–C10	3.31
C52–C11	3.27	C52–C16	3.42
C51–C7	3.46	C51–C8	3.45
C51–C9	3.66	C51–C16	3.64
C54–C14	3.59	C54–C15	3.49
C54–C16	3.66	C51–C31	3.71
C51–C32	3.36	C51–C33	3.48
C52–C33	3.47		
hydrogen bonds			
O2···N5	2.87	O2···N6	2.92

Figure 5.[21] In addition to these hydrophobic interactions, all the complexes displayed intramolecular hydrogen bonding between the oxygen atoms of the β-diketonato ligand, which is bound *trans* to the tertiary amino group of the TPA moiety, and two amide N-H groups of L (Scheme 1).

In the structure of **2**, one of the phenyl rings of the dbm^- ligand is sandwiched between the two naphthyl moieties. The dihedral angles of the phenyl groups relative to the chelating diketonato moiety were different for the included phenyl group (33.9(3)°) and the outer-sphere counterpart (23.0(3)°). This is due to the steric requirements for π–π interactions with the 1-naphthyl groups. The π–π interactions formed in the cavity are summarized in Table 1. The dihedral angles between the inserted phenyl ring and the two naphthyl groups were 11.3(7)° for the one including C7–C11 and 61.4(8)° for the one including C31–C40. This indicates that one naphthyl group is close to being parallel to the phenyl ring and the other is close to forming a T-shaped π–π interaction. As can be seen in Table 1, the included phenyl group interacts with both of the 1-naphthyl groups in the hydrophobic cavity. In this case, no π–π interactions were observed between the two 1-naphthyl moieties. The in-

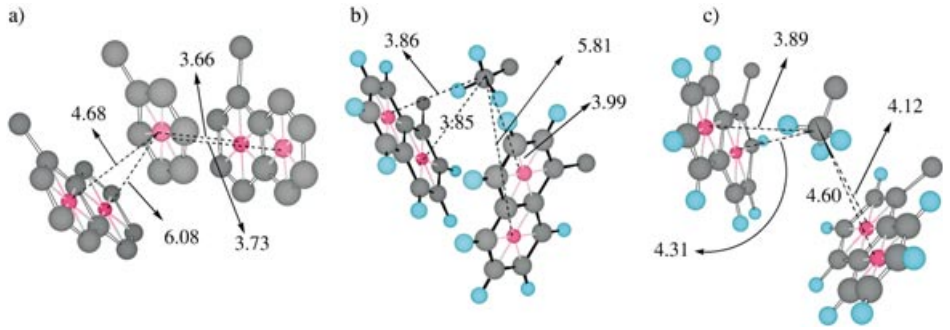

Figure 5. Distances [Å] between the included functional groups and centroids generated and estimated by Chem 3D: a) **2**, b) **3**, c) $\mathbf{4}_{Me}$.

sertion of the phenyl ring into the hydrophobic cavity in **2** is reminiscent of those observed for "molecular tweezers" reported by Zimmermann and co-workers.[22]

In the structure of **3**, one methyl group was included in the hydrophobic cavity and led to the formation of CH/π interactions; interatomic distances related to the interactions are listed in Table 2. The methyl group interacted with both of the 1-naphthyl groups as in **2**.

Table 2. Interatomic distances [Å] for intramolecular noncovalent interactions in **3**.

CH/π interactions			
C41···C14	3.59	C41···C22	3.62
C41···C23	3.45	C41···C32	3.34
C41···C33	3.52		
hydrogen bonds			
O3···N5	2.79	O3···N6	2.85

The structure of $\mathbf{4}_{Me}$ was similar to that of **3**, and all the intramolecular noncovalent interactions were consistent with those in **3**; Table 3 presents the noncovalent interactions in $\mathbf{4}_{Me}$. We could not grow crystals of $\mathbf{4}_{Ph}$; however, the included phenyl moiety should have the same structure as that in **2**, based on the results of NMR spectroscopy on the mixture of $\mathbf{4}_{Me}$ and $\mathbf{4}_{Ph}$ as mentioned above.

Table 3. Interatomic distances [Å] for intramolecular noncovalent interactions in $\mathbf{4}_{Me}$.

CH/π interactions			
C41···C21	3.38	C41···C22	3.41
C41···C31	3.51	C41···C32	3.66
C41···C40	3.64		
hydrogen bonds			
O3···N5	2.87	O3···N6	2.92

Thermal motion in 2 and 3: To shed some light on the properties of the hydrophobic cavity we examined the fluxional behavior of the included functional groups by variable-temperature (VT) NMR spectroscopy in CD_2Cl_2 in the range from 20 °C to −90 °C. In the case of **2**, the upfield-shifted signals for the phenyl group in the cavity showed good linear relationships to $1/T$ as depicted in Figure 6 (see Figure S1 in the Supporting Information). This result suggests that one mode of thermal motion is allowed for the π–π stacked moiety. In addition, the phenyl protons

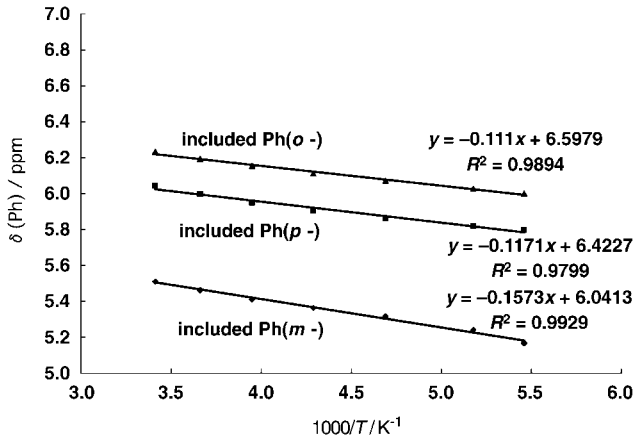

Figure 6. Temperature-dependence of the chemical shifts for signals related to π–π interactions in **2**.

showed a symmetric pattern, which indicated that the included phenyl group can rotate in the cavity. These thermal motions are retarded since we observed line broadening at lower temperatures. Thus, we assume that the allowed thermal motion is the flapping of the two 1-naphthyl arms and rotation of the phenyl ring included in the cavity.

In the case of **3**, the included methyl group (Figure 7a) exhibited two modes of thermal motion in the temperature range measured (See also Figure S2 in the Supporting Information). The singlet underwent line broadening at lower temperatures, suggesting that the free rotation was retarded, and the flapping of the two 1-naphthyl groups was also slowed down. As mentioned in the description of the molecular structure of **3**, the pseudo-triplet attributed to naphthyl proton(s) exhibited monotonic upfield shifts on lowering the temperature (Figure 7b). This observation indicates that the two naphthyl groups are allowed to exhibit one mode of thermal motion, similar to that in **2**. The intramolecular π–π interaction between the two 1-naphthyl groups, however, should not occur at higher temperatures, because it has been revealed that there is only one point of close contact, namely C24···C33 (3.60 Å) in the crystal structure.

The results described above clearly indicate that the hydrophobic cavity in the β-diketonato complexes is neither rigid nor tight and can have some flexibility to allow the phenyl ring included to *rotate freely*. Thus, this flexibility of

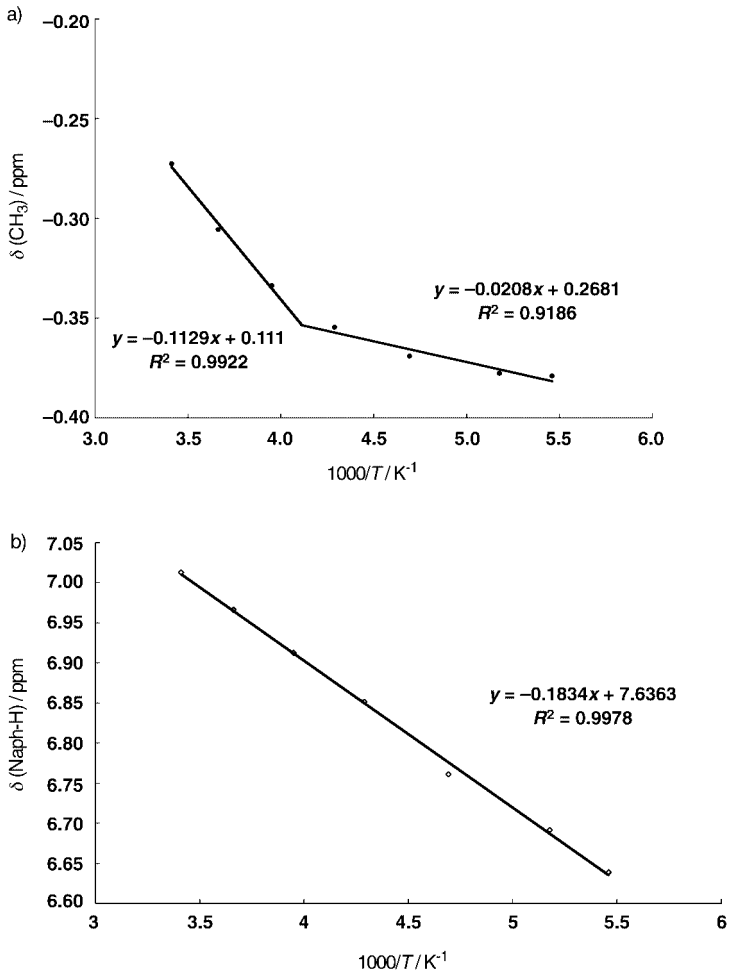

Figure 7. Temperature-dependence of the chemical shifts for the included methyl protons of the acac$^-$ ligand in **3**: a) the included methyl signal, b) a naphthyl signal.

the hydrophobic cavity will play a crucial role in the intramolecular rearrangement presented in the following section.

Intramolecular rearrangement of 4: As described above, both π–π and CH/π interactions can occur in the hydrophobic cavity consisting of the two 1-naphthyl groups. Thus, we examined the selectivity between them by using an asymmetric β-diketone, benzoylacetone (Hbac) as a ligand. In this case, the reaction proceeded smoothly as in the cases of Hdbm and Hacac to afford a mixture of two isomers of [Ru(bac)(L)]PF_6 (**4**) after 3 h as described above. Prolonged reaction at 100 °C in ethylene glycol gave only a methyl-included isomer in good yield, and its crystal structure was determined to confirm the inclusion of the methyl group (Figure 3). In the course of the reaction, however, we observed conversion of the phenyl-included isomer ($\mathbf{4_{Ph}}$) to the methyl-included isomer ($\mathbf{4_{Me}}$).

We followed the course of the reaction by monitoring the amide protons of the isomers by ^{1}H NMR spectroscopy ($\delta =$ 9.75 ppm for $\mathbf{4_{Ph}}$ and $\delta = 9.91$ ppm for $\mathbf{4_{Me}}$) in $CDCl_3$ by taking small portions of the reaction mixture in ethylene glycol. The ratio changed during the course of the reaction and $\mathbf{4_{Me}}$ became dominant and finally the sole product, that is, complete regioselectivity was observed toward $\mathbf{4_{Me}}$. We checked the order of the reaction by changing the concentration of Hbac. The conversion reaction rate was found to be $1.3\times10^{-5}\,s^{-1}$ at 100 °C in ethylene glycol and the value was independent of [Hbac] in the solution as shown in Figure 8a. This confirms that the reaction involves a one-way

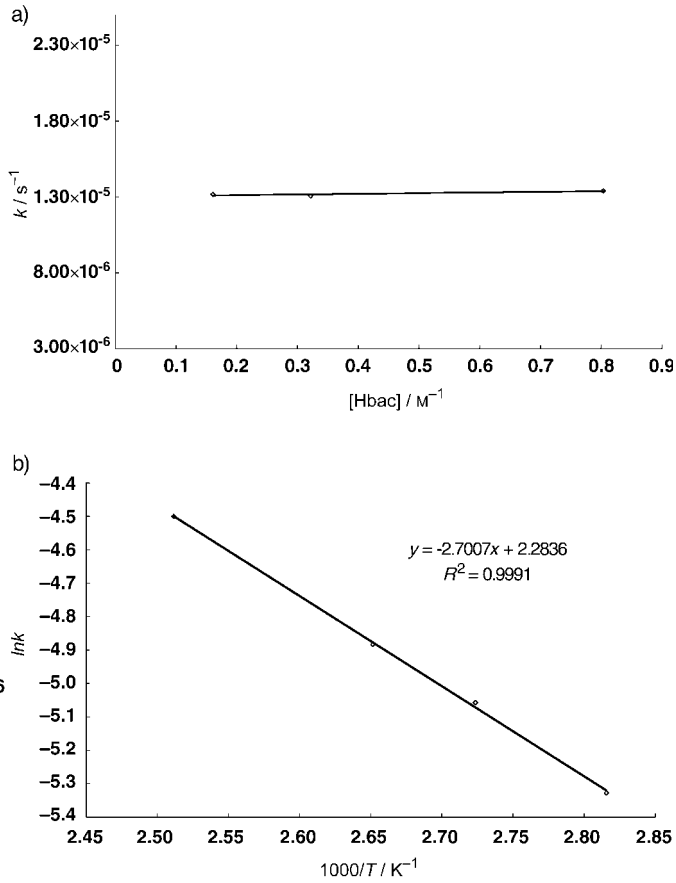

Figure 8. a) Dependence of the peudo-first-order rate constants on [Hbac], and b) an Arrhenius plot for the rearrangement in **4**.

intramolecular rearrangement of the coordinated bac$^-$ ligand to give $\mathbf{4_{Me}}$. The activation energy of this intramolecular rearrangement was determined by the use of an Arrhenius plot (Figure 8b) to be 52 kJ mol^{-1}. Thus, we propose the reaction mechanism shown in Figure 9. One-way conversion of $\mathbf{4_{Ph}}$ to $\mathbf{4_{Me}}$ indicates that $\mathbf{4_{Me}}$ is more thermodynamically stable than $\mathbf{4_{Ph}}$. Intramolecular rearrangements of Ru^{III}–β-diketonato complexes such as [Ru(β-diketonato)$_3$] in *N*,*N*-dimethylformamide have been reported, and the reaction mechanism involves a bond rupture, which depends on the nearest β-substituents.[23] In the present system, however, rupture of the Ru–O bond in the phenyl isomer cannot give the other isomer, because the coordination mode of L remains σ_h-symmetric in $\mathbf{4_{Me}}$ even when derived from $\mathbf{4_{Ph}}$ and thus the geometry of the β-diketonato complexes should be maintained. The lack of bond rupture in the rearrangement of **4** is probably due to the positive (+1) charge of **4**, which exerts a stronger electrostatic interaction with the negatively charged β-diketonato ligand, in contrast to the interaction

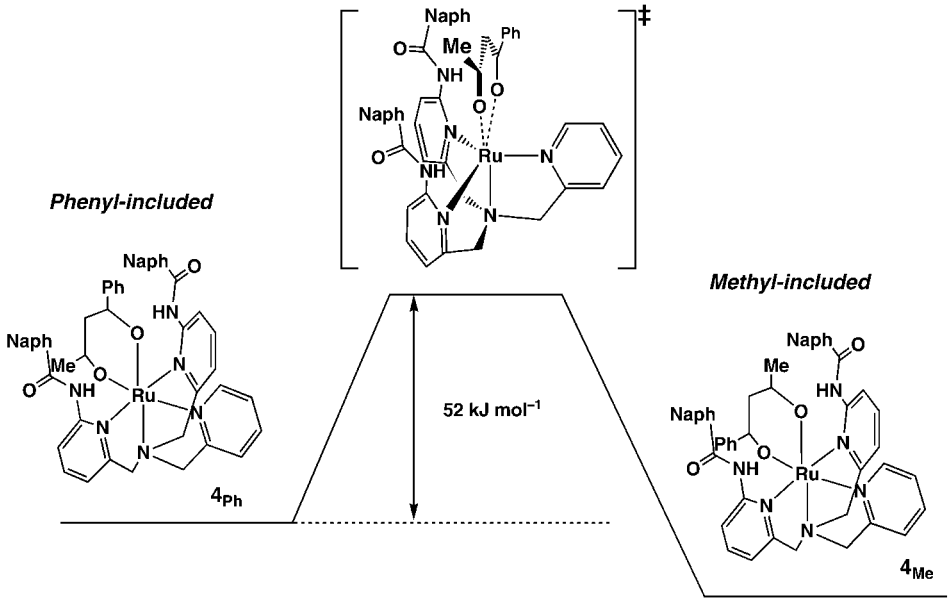

Figure 9. A proposed reaction mechanism of the intramolecular rearrangement of $\mathbf{4_{Ph}}$ to $\mathbf{4_{Me}}$ in ethylene glycol.

with the electronically neutral Ru^{III}–β-diketonato complexes mentioned above. Thus, we propose that the transition state in this intramolecular rearrangement has a peudo-trigonal bipyramidal structure with elongated Ru–O bonds (Figure 9). Intramolecular rearrangements in the coordination spheres of transition-metal complexes have been investigated; however, most of these have been regarded as rearrangements of the bonding modes of ligands.[24] On the other hand, Ru^{II} complexes have been known to form five-coordinate species[25] and to show certain flexibility around the metal center.[26]

We considered the origin of the selectivity. PM3 calculations on the bac^- ion suggested no significant difference between the negative charges on both of the oxygen atoms (−0.466 for Ph-C*O*- and −0.476 for Me-C*O*-). This result is consistent with the fact that kinetic production of $\mathbf{4_{Ph}}$ and $\mathbf{4_{Me}}$ is comparable in the initial stage (3 h of the reaction) of the β-diketonate ligation; the initial ratio of $\mathbf{4_{Me}}$:$\mathbf{4_{Ph}}$ was 1.8:1. Therefore, the kinetic control due to the negative charge on the oxygen atom is not a dominant factor in determining the selectivity.

The second candidate for the driving force of the selectivity could be steric effects. We examined a competitive reaction of **1** with an equimolar mixture of Hdbm and Hacac in ethylene glycol at 100 °C in the presence of 2,6-dimethylpyridine. This gave a mixture of **2** and **3** in the ratio of 1:4.8 after a reaction time of 24 h, indicating that the $acac^-$ ion can access the the Ru^{II} center more easily than the dbm^- ion. This result suggests that steric effects may contribute to the regioselectivity, however, it does not give complete selectivity toward **3**. Therefore, we deduce that the steric effects are not the definitive determinant for the regioselectivity observed in the formation of $\mathbf{4_{Me}}$.

The effects of solvents were examined by changing ethylene glycol to methanol and ethanol. The reaction rates increased in accordance with the elevation of the reaction temperatures, as expected in the order of methanol < ethanol < ethylene glycol. The reaction in ethylene glycol/1,2-dichloroethane (3/2 v/v) at 100 °C was examined to evaluate the character of the transition state of the rearrangement. The initial ratio (3 h) of $\mathbf{4_{Me}}$:$\mathbf{4_{Ph}}$ was 1.8:1, which was identical to that in ethylene glycol. The rate constant of the intramolecular rearrangement under these conditions was reduced by more than 10-fold ($1.8\times10^{-6}\ s^{-1}$), suggesting that the transition state of the rearrangement should be polar. This result supports the polar transition state as proposed in Figure 8, meaning that the transition state should be more ionic than the ground states.

The superiority of the CH/π interaction of the bac^- coordination was not affected by the solvent polarity. Thus, we would like to propose that the CH/π interaction can be stronger than the π–π interaction in certain cases. Yamauchi and co-workers have reported that a CH/π interaction between an N-methyl group and an uncoordinated indole moiety selectively takes place in a square-planar Pd^{II} complex, and no π–π interaction with a coordinated phenolate group occurs even in solution.[27] Polarization of the C–H bond is also important to enhance the positive character of C-*H*,[28,29] as in the case of the acetyl methyl group in $acac^-$, bac^-, and the *N*-methyl group mentioned above. From this viewpoint, we examined DFT calculations at the B3LYP/LANL2DZ level of theory to evaluate the difference in Mulliken charges of the methyl hydrogen atoms between the included and the non-included methyl groups in complex **3**.[30] The included methyl group was shown to have Mulliken charges of −0.755 for the carbon atom and +0.249, +0.246, and +0.204 for the hydrogen atoms, the former two of which are directed to the aromatic rings. The non-included methyl group exhibited Mulliken charges of −0.736 for the carbon atom and +0.227, +0.223, and +0.221 for the hydrogen atoms. Thus, the more positive charges were obtained for the included methyl hydrogen atoms than for the non-included counterpart. These results indicate that the polarization of C–H bonds is important for the strong CH/π interaction and are consistent with the results reported by Yamauchi and Aoyama and their co-workers as mentioned above.

Conclusion

We have discovered a unique intramolecular rearrangement of a β-diketonato ligand in which a one-way pseudo-rotation occurs in a Ru^{II}–TPA coordination environment comprising

a hydrophobic cavity having some flexibility. The regioselectivity in the coordination of the asymmetric β-diketonato ligand of bac⁻ is governed by the noncovalent interactions in the hydrophobic cavity. In this case, the CH/π interaction can be superior to the π–π interaction in the same hydrophobic environment, even though steric effects would be also valid. This is a significant finding with regard to the importance of the CH/π interaction in determining the chemical properties and chemoselectivity.

Experimental Section

General: Ethylene glycol, CH_2Cl_2, $CHCl_3$, MeOH, 2,6-dimethylpyridine, β-diketones (WACO Pure Chemicals Industries) were used without further purification. Et_2O was purified by distillation over Na/benzophenone. The preparation of [RuCl{(1-naph)$_2$-TPA}]PF_6·H_2O (**1**) (1-naph$_2$-TPA = *N*,*N*-bis(6,6′-(1-naphthoylamide)-2-pyridylmethyl)-*N*-(2-pyridylmethyl)amine) will be reported elsewhere.[19] NMR spectra were measured on JEOL EX-270 and GX-400 spectrometers, and UV/Vis spectra were recorded on a Jasco Ubest-55 UV/VIS spectrophotometer at room temperature. ESI mass spectra were recorded on a Perkin-Elmer Sciex API-300 mass spectrometer. All elemental analysis data were obtained at the Service Center of the Elemental Analysis of Organic Compounds, Department of Chemistry, Kyushu University.

Synthesis of [Ru(dbm){(1-naph)$_2$-TPA}](PF$_6$) (2): Compound **1** (100 mg, 0.108 mmol) was added under N_2 to a degassed solution of dibenzoylmethane (242 mg, 1.08 mmol) and 2,6-dimethylpyridine (139 mg, 1.29 mmol) in ethylene glycol (5 mL). The mixture was heated to 100 °C for 45 h under N_2 and then dried under reduced pressure. The residue was extracted with CH_2Cl_2/water and the CH_2Cl_2 layer was dried over $MgSO_4$. After the $MgSO_4$ had been removed by filtration, the solution was concentrated to a small volume and EtOH was added. The ethanolic solution was concentrated and a red precipitate emerged, which was filtered and washed with EtOH and then Et_2O. The solid was further purified by column chromatography on a silica gel column (Waco gel C-200, Waco Pure Chemicals) eluted with $CHCl_3$/MeOH (20/3 v/v). After the solvents had been removed, the solid was dissolved in a small volume of CH_2Cl_2. A brown precipitate of **2** was obtained by adding hexane to the CH_2Cl_2 solution. Yield: 69 mg, 58%. ^{1}H NMR (CD_3CN): δ = 4.50 (s, 2H; ax-CH_2-py), 4.78 and 5.27 (ABq, J = 15 Hz, 4H; eq-CH_2-py), 5.54 (t, J = 8 Hz, 2H; *m*-H of dbm⁻), 6.12 (td, J = 7 and 1 Hz, 1H; *p*-H of dbm⁻), 6.50 (dd, J = 8 and 1 Hz, 2H; *o*-H of dbm⁻), 6.71 (s, 1H; CH of dbm⁻), 8.24 (d, J = 9 Hz, 2H; naph-H2), 9.68 ppm (s, 2H; N-*H*); ^{13}C NMR ([D$_6$]acetone; selected): δ = 69.7 (ax-CH_2-), 71.4 (eq-CH_2-), 98.0 (*C*H of dbm), 168.8 (*C*O of amide), 181.6 (eq-*C*O of dbm⁻), 184.9 ppm (ax-*C*O of dbm⁻); elemental analysis calcd (%) for $C_{55}H_{43}N_6O_4RuPF_6$: C 60.16, H 3.95, N 7.65; found: C 59.95, H 3.95, N 8.11; FAB-MS: *m*/*z*: 953.3 [M^+]; absorption maxima (λ_{max}, (ε), in CH_3CN): 287 (3.2×10^4), 348 (1.8×10^4), 456 nm (sh; 1.2×10^4 M^{-1}cm^{-1}).

Synthesis of [Ru(acac){(1-naph)$_2$-TPA}](PF$_6$)·H$_2$O (3·H$_2$O): Compound **1** (100 mg, 0.108 mmol) was added under N_2 to a degassed solution of acetylacetone (60 mg, 0.60 mmol) and 2,6-dimethylpyridine (68 mg, 0.66 mmol) in ethylene glycol (5 mL). The mixture was heated to 100 °C for 45 h under N_2 and then dried under reduced pressure. After the solvent had been removed, the residue was purified by column chromatography on a silica gel column eluted with CH_2Cl_2/hexane (20/1 v/v) to obtain an yellow fraction, which was dried to remove the solvents. After the yellow solid was dissolved in CH_2Cl_2, hexane was added to obtain a yellow powder of **3**. Yield: 62 mg, 60%. Elemental analysis calcd (%) for $C_{45}H_{39}N_6O_4RuPF_6$: C 55.50, H 4.04, N 8.63; found: C 55.38, H 4.15, N 8.46; ^{1}H NMR (CD_2Cl_2): δ = −0.27 (s, 3H; included CH_3 of acac⁻), 1.86 (s, 3H; CH_3 of acac⁻), 4.47 (s, 2H; axial CH_2), 4.77 and 5.08 (Abq, 4H; eq CH_2), 5.13 (s, 1H; C*H* of acac⁻), 7.02 (t, 2H; H4 of pyr′), 7.13 (d, 2H; H5 of Naph), 7.15 (t, 1H; H3 of pyr), 7.24 (t, 1H; H5 of pyr), 7.31 (d, 2H; H5 of pyr′), 7.91 (d, 2H; H3 of pyr′), 8.02 (d, 2H; H8 of Naph), 8.04 (d, 2H; H4 of Naph), 8.22 (d, 2H; H2 of Naph), 8.95 (d, 1H; H6 of pyr), 9.89 pm (s, 2H; N*H*); absorption maxima (λ_{max}, (ε), in CH_3CN): λ = 280 (3.0×10^4), 417 (8.8×10^3), 458 nm (7.7×10^3 M^{-1}cm^{-1}).

Synthesis of [Ru(bac){(1-naph)$_2$-TPA}](PF$_6$)·H$_2$O (4·H$_2$O): Compound **1** (50 mg, 0.054 mmol) was added under N_2 to a degassed solution of benzoylacetone (87 mg, 0.54 mmol) and 2,6-dimethylpyridine (70 mg, 0.65 mmol) in ethylene glycol (5 mL). The mixture was heated to 100 °C for 24 h under N_2. Purification was carried out as described for [Ru(dbm){(1-naph)$_2$-TPA}](PF_6) to obtain a methyl-included isomer (**4$_{Me}$**) (34 mg, 61%). Elemental analysis calcd (%) for $C_{50}H_{41}N_6O_4RuPF_6$·H_2O: C 55.30, H 3.99, N 7.73; found: C 54.61, H 3.79, N 8.09; ^{1}H NMR ([D$_6$]acetone): δ = −0.16 (s, 3H; included CH_3), 4.85 (s, 2H; ax-CH_2), 5.14 and 5.46 (ABq, 4H; $J_{A,B}$ = 15 Hz), 5.96 (s, 1H; C*H* of bac⁻), 7.29–8.35 (overlapped multiplets, aromatic), 9.21 (d, 1H; 5 Hz, ax-py-H6), 9.98 ppm (s, 2H; amide-N*H*); absorption maxima (λ_{max}, (ε), in CH_3CN): 287 (3.0×10^4), 313 (1.9×10^4), 439 nm (1.1×10^4 M^{-1}cm^{-1}).

X-ray crystallographic data of 2: Single crystals of **2** were obtained by recrystallization from CH_2Cl_2/EtOH. A dark red (brown) crystal ($0.10\times0.17\times0.16$ mm^3) was mounted on a glass fiber. All measurements were made on a Rigaku RAXIS-RAPID Imaging Plate diffractometer with graphite-monochromated $Mo_{K\alpha}$ (λ = 0.7107 Å) radiation. Indexing was performed from three oscillations that were exposed for 3.0 min. The data were collected at −140 ± 1 °C to a maximum 2θ value of 54.8°. The exposure time was 2.5 min per degree. Data were processed by using the PROCESS-AUTO program package. A symmetry-related absorption correction was applied, and the data were corrected for Lorentz polarization effects.

The structure was solved and refined by direct methods by using the SHELXS-97 program package.[31] Owing to the poor quality of the crystals, structure refinements were done by using both isotropic and anisotropic thermal factors. Crystal data for **2**: $C_{63.50}H_{51}N_6O_6F_6PRu$, triclinic, space group $P\bar{1}$, a = 11.264(2), b = 15.503(3), c = 17.315(4) Å, α = 95.49(3), β = 106.36(3), γ = 106.36(3)°, V = 2732.7(10) Å^3, Z = 2, ρ_{calcd} = 1.507 g cm^{-1}, T = 133 K, $R1$ ($I > 2\sigma(I)$) = 0.100, Rw = 0.298 (all data). GOF = 1.12.

X-ray crystallographic data of 3: Single crystals of **3** were obtained by recrystallization from CH_3CN. A yellow crystal ($0.10\times0.20\times0.30$ mm^3) was mounted on a glass fiber. All measurements were made on a Rigaku RAXIS-RAPID Imaging Plate diffractometer with graphite-monochromated $Mo_{K\alpha}$ (λ = 0.7107 Å) radiation. Indexing was performed from three oscillations that were exposed for 3.0 min. The data were collected at −160 ± 1 °C to a maximum 2θ value of 55.0°. The exposure time was 2.0 min per degree. Data were processed by using the PROCESS-AUTO program package. A symmetry-related absorption correction was applied and the data were corrected for Lorentz polarization effects.

The structure was solved by direct methods and expanded by using Fourier techniques. All non-hydrogen atoms were refined anisotropically and hydrogen atoms were included but not refined. The atomic scattering factors were taken from reference [32], and anomalous dispersion effects were included as mentioned above. All calculations were performed by using the teXsan crystallographic software package.[33] Crystal data for **3**: triclinic, space group $P\bar{1}$, a = 16.6266(4), b = 16.7229(5), c = 19.3806(9) Å, α = 76.724(2), β = 64.458(5), γ = 75.606(2)°, V = 4663.0(3) Å^3, Z = 2, ρ_{calcd} = 1.433 g cm^{-1}, T = 113 K, $R1$ ($I > 2\sigma(I)$) = 0.131, Rw = 0.169, GOF = 1.90.

X-ray crystallographic data of 4$_{Me}$: Single crystals of **4$_{Me}$** were obtained by recrystallization by vapor deposition of EtOAc onto a solution of **4$_{Me}$** in CH_3CN. A red crystal was mounted on a glass fiber. All measurements were made on a Rigaku RAXIS-RAPID Imaging Plate diffractometer with graphite-monochromated $Mo_{K\alpha}$ (λ = 0.7107 Å) radiation. Indexing was performed from three oscillations that were exposed for 3.0 min. The data were collected at −140 ± 1 °C to a maximum 2θ value of 55.0°. The exposure time was 2.0 min per degree. Data were processed by using the PROCESS-AUTO program package. A symmetry-related absorption correction was applied and the data were corrected for Lorentz polarization effects.

The structure was solved by direct methods and expanded by using Fourier techniques. All non-hydrogen atoms were refined anisotropically and hydrogen atoms were included but not refined. The atomic scattering factors were taken from ref. [21], and anomalous dispersion effects were included as mentioned above. All calculations were performed by using the teXsan crystallographic software package. Crystal data for **4$_{Me}$**: monoclinic, space group $P2_1/c$, a = 8.950(1), b = 14.083(2), c = 38.223(4) Å, β =

92.624(8)°, $V = 4812(1)$ Å^3, $Z = 4$, $\rho_{calcd} = 1.430$ g·cm^{-1}, $T = 133$ K, $R1$ ($I > 3\sigma(I)$) = 0.098, $Rw = 0.250$, GOF = 1.96.

CCDC-235948 ($\mathbf{4_{Me}}$), CCDC-235949 (**2**), and CCDC-235950 (**3**) contain the supplementary crystallographic data for this paper. These data can be obtained free of charge via www.ccdc.cam.ac.uk/conts/retrieving.html (or from the Cambridge Crystallographic Data Centre, 12 Union Road, Cambridge CB21EZ, UK; fax: (+44)1223-336-033; or deposit@ccdc.cam.ac.uk).

Kinetic study on the intramolecular rearrangement of 4: A mixture of **1** (1.5×10^{-2} mol L^{-1}) and Hbac (1.5×10^{-1} mol L^{-1}) in ethylene glycol in the presence of 2,6-dimethylpyridine (1.5×10^{-1} mol L^{-1}) was heated at 100 °C under air. At the appropriate reaction time, a small volume of the mixture was taken and dried in vacuo and then dissolved into $CDCl_3$ for ^{1}H NMR measurements. After the signals for **1** had disappeared, the intramolecular rearrangement was monitored by the integration of the amide NH signals of $\mathbf{4_{Me}}$ and $\mathbf{4_{Ph}}$. The integration ratio was used to determine the rate constant of the intramolecular rearrangement. To obtain an Arrhenius plot for the reaction, the reaction was carried out at 82 °C (355.15 K), 94 °C (367.15 K), 104 °C (377.15 K), and 125 °C (398.15 K), to determine the rate constant at each temperature.

Acknowledgement

We are grateful to Dr. Masaki Kawano (The University of Tokyo) for his help with the X-ray crystallography and to Prof. Teruo Shinmyouzu (Institute of Materials Chemistry and Engineering, Kyushu University) for allowing us the use the X-ray diffractometer. We thank Ms. Kayoko Ogi (Center for Elemental Analysis of Organic Compounds, Kyushu University) for her expertise in VT NMR measurements. We are also grateful to Prof. Kazunari Yoshizawa and Dr. Yoshihito Shiota (Institute of Materials Chemistry and Engineering, Kyushu University) for performing the DFT calculations. We also thank Prof. Shunichi Fukuzumi (Osaka University) for providing useful comments. This work was partially supported by a Grant-in-Aid (11740373 to T. K.) from The Ministry of Education, Culture, Sports, Science and Technology of Japan.

[1] J. W. Steed, J. L. Atwood, *Supramolecular Chemistry*, Wiley, Chichester, **2000**.
[2] a) M. Nishio, M. Hirota, *Tetrahedron* **1989**, *45*, 7201–7245; information on CH/π interactions is available at http://www.tim.hi-ho.ne.jp/dionisio.
[3] a) C. A. Hunter, J. K. M. Sanders, *J. Am. Chem. Soc.* **1990**, *112*, 5525–5534; b) C. Janiak, *J. Chem. Soc. Dalton Trans.* **2000**, 3885–3896.
[4] E. A. Meyer, R. K. Castellano, F. Diederich, *Angew. Chem.* **2003**, *115*, 1244–1287; *Angew. Chem. Int. Ed.* **2003**, *42*, 1210–1250.
[5] a) R. Harada, Y. Matsuda, H. Okawa, T. Kojima, *Angew. Chem.* **2004**, *116*, 1861–1864; *Angew. Chem. Int. Ed.* **2004**, *43*, 1825–1828; b) H. Uno, A. Matsumoto, N. Ono, *J. Am. Chem. Soc.* **2003**, *125*, 12082–12083; c) T. Yamaguchi, N. Ishii, K. Tashiro, T. Aida, *J. Am. Chem. Soc.* **2003**, *125*, 13934–13935.
[6] a) A. J. Goshe, I. M. Steele, C. Ceccarelli, A. L. Rheingold, B. Bosnich, *Proc. Natl. Acad. Sci. USA* **2002**, *99*, 4823–4829; b) R. D. Sommer, A. L. Rheingold, A. J. Goshe, B. Bosnich, *J. Am. Chem. Soc.* **2001**, *123*, 3940–3952; c) C. Janiak, L. Uelin, H. -P. Wu, P. Klüfers, H. Piotrowski, T. G. Scharmann, *J. Chem. Soc. Dalton Trans.* **1999**, 3121–3131.
[7] a) F. -G. Klärner, B. Kahlert, *Acc. Chem. Res.* **2003**, *36*, 919–932, and references therein; b) J. W. Lee, S. Samal, N. Selvaparam, H. -J. Kim, K. Kim, *Acc. Chem. Res.* **2003**, *36*, 621–630.
[8] For example: C. A. Claussen, E. C. Long, *Chem. Rev.* **1999**, *99*, 2797–2816.
[9] H. Sakamoto, M. S. Lewis, H. Kodama, E. Appella, K. Sakaguchi, *Proc. Natl. Acad. Sci. USA* **1994**, *91*, 8974–8978.
[10] K. Sakaguchi, I. Ito, Y. Shimohigashi, *Peptide Science* **2001**, 277–280.
[11] G. Ujaque, P. S. Lee, K. N. Houk, M. F. Hentemann, S. J. Damishefsky, *Chem. Eur. J.* **2002**, *8*, 3423–3430, and references therein.
[12] a) O. Yamauchi, A. Odani, M. Takani, *J. Chem. Soc. Dalton Trans.* **2002**, 3411–3421, and references therein; b) O. Yamauchi, A. Odani, S. Hirota, *Bull. Chem. Soc. Jpn.* **2001**, *74*, 1525–1545; c) H. Ôkawa, *Coord. Chem. Rev.* **1988**, *92*, 1–28, and references therein; d) S. K. Chowdhury, V. S. Joshi, A. G. Samuel, V. G. Puranik, S. S. Tavale, A. Sarkar, *Organometallics* **1994**, *13*, 4092–4096.
[13] R. Noyori, M. Yamakawa, S. Hashiguchi, *J. Org. Chem.* **2001**, *66*, 7931–7944, and references therein.
[14] a) F. Zhang, A. Odani, H. Masuda, O. Yamauchi, *Inorg. Chem.* **1996**, *35*, 7148–7155; b) T. Sugimori, K. Shibakawa, H. Masuda, A. Odani, O. Yamauchi, *Inorg. Chem.* **1993**, *32*, 4951–4959; c) A. Odani, S. Deguchi, O. Yamauchi, *Inorg. Chem.* **1986**, *25*, 62–69; c) O. Yamauchi, A. Odani, *J. Am. Chem. Soc.* **1985**, *107*, 5938–5945.
[15] a) E. Dubler, U. K. Häring, K. H. Scheller, P. Baltzer, H. Sigel, *Inorg. Chem.* **1984**, *23*, 3785–3792; b) H. Sigel, K. H. Scheller, R. M. Milburn, *Inorg. Chem.* **1984**, *23*, 1933–1938; c) K. H. Scheller, H. Sigel, *J. Am. Chem. Soc.* **1983**, *105*, 3005–3014; d) B. E. Fisher, H. Sigel, *J. Am. Chem. Soc.* **1980**, *102*, 2998–3008.
[16] H. Okawa, K. Ueda, S. Kida, *Inorg. Chem.* **1982**, *21*, 1594–1598.
[17] H. Okawa, T. Katsuki, M. Nakamura, N. Kumagai, Y. Shuin, T. Shinmyozu, S. Kida, *J. Chem. Soc. Chem. Commun.* **1989**, 139–140.
[18] T. Kojima, K. Hayashi, Y. Matsuda, *Chem. Lett.* **2000**, 1008–1009.
[19] T. Kojima, K. Hayashi, Y. Matsuda, *Inorg. Chem.* **2004**, *43*, 6793–6804.
[20] T. Kojima, T. Amano, Y. Ishii, M. Ohba, Y. Okaue, Y. Matsuda, *Inorg. Chem.* **1998**, *37*, 4076–4085.
[21] C. Janiak, S. Temizdemir, S. Dechert, W. Deck, F. Girgsdies, J. Heinze, M. J. Kolm, T. G. Scharmann, O. M. Zipffel, *Eur. J. Inorg. Chem.* **2000**, 1229–1241.
[22] a) S. C. Zimmermann, C. M. VanZyl, *J. Am. Chem. Soc.* **1987**, *109*, 7894–7896; b) S. C. Zimmermann, M. Mrksich, M. Baloga, *J. Am. Chem. Soc.* **1989**, *111*, 8528–8530; c) S. C. Zimmermann, C. M. VanZyl, G. S. Hamilton, *J. Am. Chem. Soc.* **1989**, *111*, 1373–1381; d) S. C. Zimmermann, Z. Zeng, W. Wu, D. E. Reichert, *J. Am. Chem. Soc.* **1991**, *113*, 183–196; e) S. C. Zimmermann, W. Wu, Z. Zeng, *J. Am. Chem. Soc.* **1991**, *113*, 196–201; f) H. M. Whitlock, Jr., C. W. Chen, *J. Am. Chem. Soc.* **1978**, *100*, 4921–4922.
[23] Y. Hoshino, R. Takahashi, K. Shimizu, G. P. Sato, K. Aoki, *Inorg. Chem.* **1990**, *29*, 4816–4820.
[24] R. H. Fish, H. -S. Kim, R. H. Fong, *Organometallics* **1991**, *10*, 770–770.
[25] a) P. Steenwinkel, S. L. James, R. A. Gossage, D. M. Grove, H. Kooijman, W. J. J. Smeets, A. L. Spek, G. van Koten, *Organometallics* **1998**, *17*, 4680–4693; b) P. González-Herrero, B. Weberndörfer, K. Ilg, J. Wolf, H. Werner, *Angew. Chem.* **2000**, *112*, 3392–3395; *Angew. Chem. Int. Ed.* **2000**, *39*, 3266–3269; c) D. G. Gusev, A. J. Lough, *Organometallics* **2002**, *21*, 5091–5099.
[26] S. T. Wilson, J. A. Osborn, *J. Am. Chem. Soc.* **1971**, *93*, 3068–3070.
[27] T. Yajima, Y. Shimazaki, N. Ishigami, A. Odani, O. Yamauchi, *Inorg. Chim. Acta* **2002**, *337*, 193–202.
[28] K. Kobayashi, Y. Asakawa, Y. Kikuchi, H. Toi, Y. Aoyama, *J. Am. Chem. Soc.* **1993**, *115*, 2648–2654.
[29] The acidic alkynyl hydrogen atom can also be a good CH/π donor: H. -C. Weiss, D. Bläser, R. Boese, B. M. Doughan, M. M. Haley, *Chem. Commun.* **1997**, 1703–1704.
[30] a) A. D. Becke, *Phys. Rev. A* **1988**, *38*, 3098–3100; b) A. D. Becke, *J. Chem. Phys.* **1993**, *98*, 5648–5652; c) C. Lee, W. Yang, R. G. Parr, *Phys. Rev. B* **1988**, *37*, 785–789; d) T. H. Dunning, Jr., P. J. Hay in *Modern Theoretical Chemistry*, (Ed.: H. F. Schaefer, III), Plenum, New York, **1976**; e) P. J. Hay, W. R. Wadt, *J. Chem. Phys.* **1985**, *82*, 299–310.
[31] G. M. Sheldrick, SHELXS-97, A software package for the solution and refinement of X-ray data, University of Göttingen, Göttingen, Germany.
[32] D. T. Cromer, J. T. Waber, *International Tables for X-ray Crystallography*, vol. IV; Kynoch Press: Birmingham, England; Table 2.2 A, **1974**.
[33] teXsan: Crystal Structure Analysis Package, Molecular Structure Corporation, **1985** and **1999**.

Received: May 19, 2004
Published online: November 5, 2004

